

Pathways to interstellar amides via carbamoyl (NH₂CO) isomers by radical-neutral reactions on icy-grains

Gabriela Silva-Vera,[†] Giulia M. Bovolenta,^{†,¶} Namrata Rani,[‡] Sebastian Vera,[†]
and Stefan Vogt-Geisse^{*,‡}

[†]*Departamento de Fsico-Qumica, Facultad de Ciencias Qumicas, Universidad de
Concepcin, 4070386 Concepcin, Chile*

[‡]*Departamento de Fsico-Qumica, Facultad de Ciencias Qumicas, Universidad de
Concepcin, 4070386 Concepcin, Chile*

[¶]*Atomistic Simulations, Italian Institute of Technology, 16152 Genova, Italy*

E-mail: stvogtgeisse@qcmmlab.com

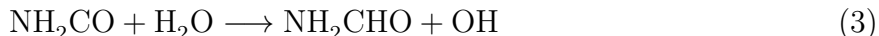
Abstract

Explaining the formation pathways of amides on ice-grain mantels is crucial to the understanding of prebiotic chemistry in the interstellar medium. In this computational study, we explore different radical-neutral formation pathways for some of the observed amides (formamide, acetamide, urea and N-methylformamide) via intermediate carbamoyl (NH_2CO) radical precursor and its isomers. We assess the relative energy of four NH_2CO isomers in the gas phase and evaluate their binding energy on small water clusters to discern the affinity that the isomers present to a ice model. We consider three possible reaction pathways for the formation of the carbamoyl radicals, namely the $\text{OH} + \text{HCN}$, $\text{CN} + \text{H}_2\text{O}$ and $\text{NH}_2 + \text{CO}$ reaction channels. We computed the binding energy distribution for the HCN and CH_3CN precursors on a ice model consisting of a set-of-clusters of 22-water molecules each, to serve as a starting point to the reactivity study on the ice surface. The computations revealed that the lowest barrier to the formation of a NH_2CO isomer corresponds to the $\text{NH}_2 + \text{CO}$ reaction (12.6 kJ mol^{-1}). The reaction pathway $\text{OH} + \text{HCN}$ results in the exothermic formation of the N-radical form of the carbamoyl $\text{HN}(\text{C}=\text{O})\text{H}$ with a reaction barrier of 26.7 kJ mol^{-1} . We found that the $\text{CN} + \text{H}_2\text{O}$ reaction displays a high energy barrier of 70.6 kJ mol^{-1} . Finally, we also probed the direct formation of acetamide radical precursor via the $\text{OH} + \text{CH}_3\text{CN}$ reaction, and found that the most probable outcome on interstellar ices is the H-abstraction reaction to yield CH_2CN and H_2O . Based on those result, we believe that including alternative reactions pathways, leading to the formation of amides via the N-radical form of carbamoyl, would provide an improvement in the prediction of the amides abundances in astrochemical models, especially regarding chemistry of star-forming regions.

1 Introduction

Despite its overreaching emptiness, the interstellar medium (ISM) harbors gas, dust, and organic compounds. This space includes molecular clouds, which are colder, denser areas with temperatures ranging from 10 to 30 K and particle densities between 10^4 and 10^8 particles per cubic centimeter. Under these frigid conditions, gas-phase molecules adhere to dust grains - composites of non-volatile materials like carbon-based substances, oxides, and silicates - forming an icy mantle. Such ice mantles are rich in water and also contain a mix of simple molecules, including CO_2 , CO , CH_4 and NH_3 .¹ The formation of interstellar complex organic molecules (iCOMs) is believed to take place on the surface of the ice mantles. Among the iCOMs, amides are prebiotic compounds characterized by a carbonyl group bonded to a nitrogen atom ($\text{R} - \text{C}(=\text{O}) - \text{N} - \text{R}'$). This structural characteristic, known as a peptide bond, is fundamental for the formation of life's building blocks like amino acids.² The majority of the observations of interstellar amides have been made towards star-forming regions.³⁻⁶ Recently, the results of a sensitive spectral survey⁷ carried out towards the quiescent molecular cloud G+0.693-0.027 revealed a rich amide inventory. They found evidence of the presence of the simplest amides, such as formamide (NH_2CHO), acetamide ($\text{CH}_3\text{C}(\text{O})\text{NH}_2$), N-methylformamide (CH_3NHCHO) and urea ($\text{NH}_2\text{C}(\text{O})\text{NH}_2$), while the quest for more complex amides is still ongoing in that as well as in other interstellar regions.^{4,8,9} Another notable result from the latest survey,⁷ was that the relative abundances of amides, when compared to formamide, typically exhibit the least difference across the different source environments, with variations frequently not exceeding a factor of five. That implies that the chemical processes responsible for the amides generation are established early in molecular cloud evolution and are not altered during the star-forming processes, suggesting that to better understand amides formation, attention should be directed toward cold cloud conditions. In such environments, amides formation might take place on the surface of interstellar icy-grains.^{10,11} Moreover, the constant column density ratios between the species suggests that similar, or linked, chemical pathways might be responsible for the

formation of the observed amides. Carbamoyl radical (NH_2CO) is considered a common precursor to interstellar amides.^{12–15} This particular species has received considerable attention due to its involvement in various straightforward synthetic pathways employed for the generation of amides. Starting from carbamoyl, formamide might be produced either by hydrogenation (1), disproportionation (2) or reaction with water (3), however, the feasibility of Reaction 1 has long been debated:^{16,17}



Addition of CH_3 and NH_2 to the carbamoyl radical leads to the formation of acetamide (4) and urea (5), respectively:



Reaction 4 has been proposed⁶ as a potential reaction pathway linking the formation of formamide and acetamide, but the process has not been investigated so far. On the other hand, both experimental¹⁴ and computational¹⁸ studies have identified Reaction 5 as a particularly promising pathway.

The generation and availability of carbamoyl radical NH_2CO in the ISM is still object of study. Possible formation pathways^{19–21} are radical addition of NH_2 to CO (6), H-abstraction from formamide (7), hydrogenation of HNCO (8), and hydration of CN (9):





Reaction 6 has been suggested based on experimental results,^{15,22,23} in which different ice-mixtures of $\text{CO}:\text{NH}_3$ and $\text{H}_2\text{O}:\text{CO}:\text{NH}_3$ are exposed to vacuum ultraviolet photons in an ultra-high vacuum chamber at 10 K. Chuang et al.¹⁵ found that the highest yields of formamide are obtained when including H_2O in the ice mixture, suggesting an important role of water in facilitating the formation reactions. On the other hand, the route involving HCN/CN has also been experimentally probed by energetic processing of $\text{HCN}:\text{H}_2\text{O}$ ice²⁴ in which formamide and HNCO were identified. This reaction pathway has also been studied theoretically using a 33-water molecules cluster as ice model.²⁵

Carbamoyl radical also presents several isomers, reported in Fig. 1, although it is unclear how these species differ in term of reactivity and stability. Among them, $\text{HN}(\text{C}=\text{O})\text{H}$, (Fig. 1, Is2), whose addition to CH_3 radical leads to the formation of N-methylformamide (10):



Analogously to carbamoyl, $\text{HN}(\text{C}=\text{O})\text{H}$ can be formed via radical recombination ($\text{NH} + \text{HCO}$), or H-abstraction from formamide.^{14,19,21}

When adsorbed on ice mantles, carbamoyl isomer are thought to convert between each other via tautomerization, so that potentially each of them could act as intermediate in the formation of several amides, as well. The tautomerization (11) of $\text{H}(\text{N}=\text{C})\text{OH}$ isomer to carbamoyl (Is4 to Is1 respectively) has been investigated using an ice model,²⁵ but the barrier for the reaction was found to be too high to take place in the coldest regions on the ISM, unless the process takes place following previous exothermic reactions, such that it might absorb the energy released by them:



Interstellar ices are primarily composed of water in amorphous form (ASW);²⁶ interstellar species interact with ASW in different ways, due to the complex hydrogen bond (H-bond) network present on the ice surface. The binding energy (BE) of a species is a measure of the strength of its interaction with the surface, and can provide information about its residency time and consequent availability to reactive encounters with other species. According to experimental and theoretical studies, the collection of BE for a certain species, considering the most complete set of binding sites on the ice, adds up to constitute a Gaussian BE distribution.^{27–30} The ASW H-bond network may also affect surface processes, enabling or disfavoring certain chemical reactions in specific ways. Therefore, adopting a realistic ice model is essential to gain insight on the surface formation routes of carbamoyl, and its isomers, and consequently elucidating the origin of interstellar amides.

A pathway not yet explored for the generation of carbamoyl on the ASW surface, is the addition reaction of hydroxyl radical (OH) to the common interstellar precursor HCN:



Reaction 12 yields the imidic acid isomer of carbamoyl (HC(OH)N, Fig. 1, Is3). Gas-phase studies for this reaction have shown that the addition pathway of OH radicals to HCN has significantly lower barrier than the competitive H-abstraction:^{31,32}



When OH is added to CH₃CN species instead, the reaction yields the corresponding acetamide precursor radical:



Moreover, OH radicals can be easily produced in interstellar conditions, not only by the photolysis and/or ion bombardments of H_2O but also the reaction of H and O atoms,^{33,34} so that they are thought to be one of the most abundant radicals on ice dust.³⁵

In this work, we present an estimation of the BE range and relative energetic stability of the census of the isomers of carbamoyl radical, adsorbed on a minimal ice model, constituted of clusters of up to 5 water molecules each. We propose the first exploration of the HCN and $\text{CH}_3\text{CN} + \text{OH}$ addition pathways (Reactions 12, 14) on a ASW surface model composed of 22-water molecules, as a synthetic route to NH_2CO and $\text{CH}_3\text{C}(\text{OH})\text{N}$ amides precursors. The study is carried out by means of Density Functional Theory (DFT), using the BE distribution of HCN and CH_3CN adsorbed on ASW, as a starting point to select possible catalytic sites for the reaction. The prospective binding sites of HCN and CH_3CN are sampled with their reaction partner OH, in order to find viable reaction pathways. Lastly, we applied the same protocol to the analysis of the most exploited surface synthetic routes for the production of carbamoyl isomers, namely the radical addition of NH_2 to CO and of CN to H_2O (Reactions 6 and 7, respectively), as well.

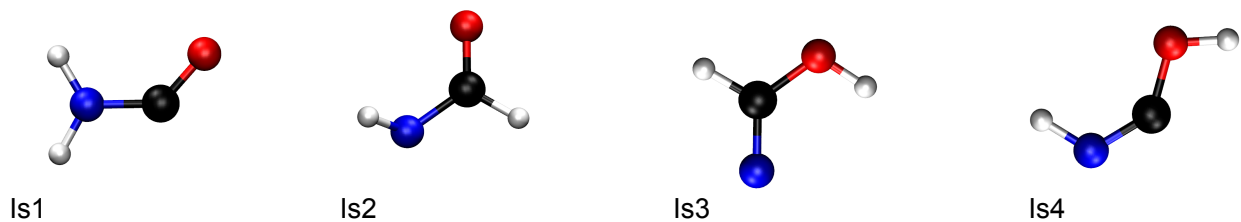


Figure 1: Carbamoyl radical, Is1 and three of its isomers, Is(2-4). The color scheme for the atoms is red for O, black for C, blue for N and white for H.

2 Computational details

2.1 ASW modeling

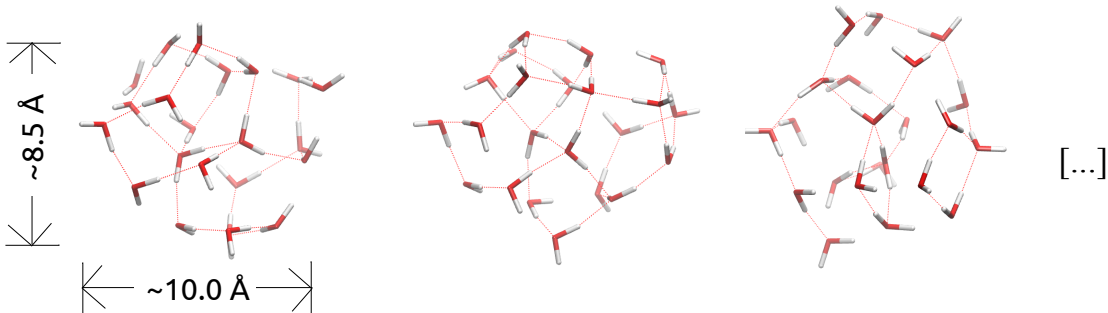


Figure 2: This work utilizes a selection of 17 homogeneous amorphous clusters, each containing 22 water molecules, for evaluating binding energies and investigating reactivity. Following modeling using AIMD techniques, the structures undergo geometry optimization. The color scheme for the atoms is red for O and white for H.

We used the 22-water molecules set-of-clusters model, which is part of the binding energy evaluation platform³⁶ (BEEP) to find suitable binding sites for the addition reactions. This model consists of 17 homogeneous amorphous clusters that are extracted from an *ab initio* MD simulation of a singular cluster containing 22 water molecules. Three examples of the clusters are shown in Fig. 2. The details about the simulation procedure can be found elsewhere.³⁰ As each of the 17 clusters represent unique fragments of ASW surface, the set-of-cluster encompass a rich variety of binding sites, thus providing many possible sites that could be susceptible to reactive encounters.

2.2 Binding Energy and Binding Energy Distributions

The binding energy of a species (i) adsorbed on a surface (ice) is defined as:

$$BE(i) = E_{sup} - (E_{ice} + E_i) \tag{15}$$

where E_{sup} stands for the energy of the supermolecule formed by the adsorbate bound to the surface, E_{ice} refers to the surface energy, and E_i is the energy of the adsorbate. The BE is assumed to be a positive quantity, according to convention. Using a BE distribution of values reflects a more realistic desorption behavior for molecules adsorbed on ASW ice. The binding energy distributions of HCN and CH₃CN are computed using using BEEP computational platform and protocol^{36a}. The performance of DFT largely depends on the exchange-correlation density functionals employed. Certain functionals are tailored for specific systems or optimized to accurately reproduce geometries or energy barriers. Additionally, these functionals differ significantly in computational cost. Common practice involves testing (benchmarking) a range of DFT functionals and basis sets on minimal surface models to identify the most suitable method for application to larger systems.³⁷ Therefore, the level of theory selected in this study is based on a extensive DFT geometry and energy benchmark carried out in a previous work.³⁶ The geometries of the binding sites have been computed using HF-3c method coupled with MINIX basis set³⁸ while MPWB1K³⁹ coupled with def2-TZVP⁴⁰ is used for the binding energies.

Dispersion effects are treated using D3BJ correction.⁴¹ TERACHEM⁴² and PSI4⁴³ softwares are used for the optimization of the binding sites and PSI4 for binding energy computations. BEEP is powered by the QCArchive⁴⁴ software stack.

2.3 PES exploration with QCExplore

For the exploration of the PES we employed our newly developed QCExplore platform that automatizes the search for possible reactive complexes on the ASW surface and streamlines the search for transition state structures. It consists of four pillars: prospective reactive binding site sampling with target molecule, transition path search by means of relaxed scan or nudge elastic band calculations, transition state characterization, by computing the Hessian and analyzing the normal mode frequency and displacing and relaxing the TS geometry along

^a<https://github.com/QCMM/BEEP>

the reactive normal modes with imaginary frequency, to corroborate that the TS corresponds to the correct reactants and products. Finally, the workflow also allows to compute the reaction and transition state energies at various DFT levels of theory. QCExplore is powered by the QCArchive software stack, as well. The source code of QCExplore can be found on GitHub^b. Within QCExplore, we use TERACHEM together with geomeTRIC⁴⁵ for the geometry optimizations of reactants and transition states using BHandHLYP⁴⁶ and def2-SVP. The relaxed scan and NEB computations are also done with TERACHEM/geomeTRIC. Finally the energies of the stationary points are computed with Psi4 using BMK⁴⁷ coupled with def2-TZVP basis, including D3BJ correction.

2.4 Sampling of prospective binding sites.

The procedure to identify the reactant configuration for the reactions carried out on ASW is the following:

- Selection of prospective binding sites of one of the reactive partners adsorbed on ASW (HCN for R1, H₂O for R2, NH₂ for R3 and CH₃CN for R4)
- Extensive sampling with the other fragment: the sampling procedure creates a large number (10-15) of potential reaction sites, where the fragment is arranged on a semi-spherical grid around the adsorbed species. Each generated configuration is optimized and a suitable reactant complex is chosen to study the reaction. The radius of the hemisphere is 3 Å.

3 Results and Discussion

This section is organised as follow: first, we present the analysis of the structural parameters and relative energies of carbamoyl isomers (Sec.3.1) and their BE range (Sec. 3.2). Then, we present the reactivity results for the generation of NH₂CO radicals, in gas-phase and on

^b<https://github.com/QCMM/QCExplore>

ASW for the Reaction of OH + HCN (Sec.3.3.1,3.3.2), CN + H₂O (Sec. 3.3.3), NH₂ + CO (Sec. 3.3.4). Finally, we describe the results of the reaction of OH + CH₃CN (Sec. 3.3.6). The BE distribution and binding mode analysis of HCN and CH₃CN adsorbed on ASW are displayed at the beginning of the corresponding sections (Sec. 3.3.2, 3.3.6).

3.1 Structural parameters and relative energies of carbamoyl isomers

We selected the four most common radical isomers with formula NH₂CO, Table 1 reports their structural parameters. The species share the same backbone, and differ based on the position of the H-atoms. Is1 (C-radical carbamoyl, or simply carbamoyl) and Is2 (N-radical carbamoyl) present a carbonyl group, which is reflected in the shorter distance of the C–O bond (B(N–C) is 1.20, 1.23 Å, respectively). Is2 is the most strained isomer, with a N–C–O angle value of 123.7 °. Is3 is a imidic acid, characterized by the presence of both a C=N bond and a OH group. Lastly, Is4 represents the straight-chain isomer, as indicated by the largest N–C–O angle value (132.5 °). In its lowest energy conformation, the N–H and O–H groups in Is4 are pointing in opposite directions.

Table 1: Structural parameters of carbamoyl (Is1) and its isomers (Is2-4). Geometries are obtained at UCCSD(T)-F12/cc-pVDZ-F12 level of theory. Bond distances (B) are in angstrom (Å), bond angles (A) are in degrees (°).

Isomer	B(N–C)	B(C–O)	A(N–C–O)
Is1	1.34	1.20	129.6
Is2	1.38	1.23	123.7
Is3	1.26	1.38	125.5
Is4	1.23	1.35	132.5

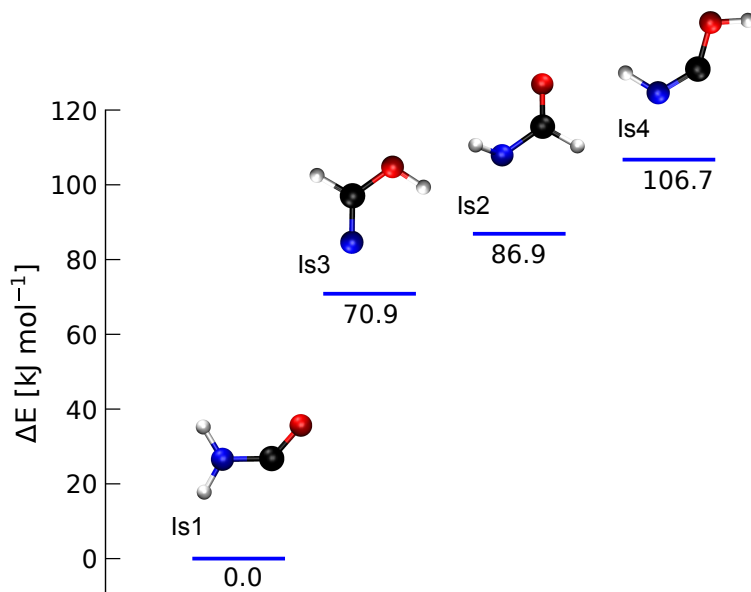


Figure 3: Relative energy of the radical isomers studied in this work, with respect to carbamoyl (Is1). Energies and geometries are computed at UCCSD(T)-F12/cc-pVDZ-F12⁴⁸ level of theory.

Fig. 3 display the relative energies of the different isomers with respect to carbamoyl (Is1). The following isomers in order of stability appears to be the imidic acid (Is3), and the N-radical form of the amide radical (Is2) with a energy difference of 70.9 and 86.9 kJ/mol, respectively. The least stable species is the linear iminic acid isomer (Is4), 106.7 kJ/mol higher in energy than carbamoyl.

3.2 Binding energy range of carbamoyl isomers

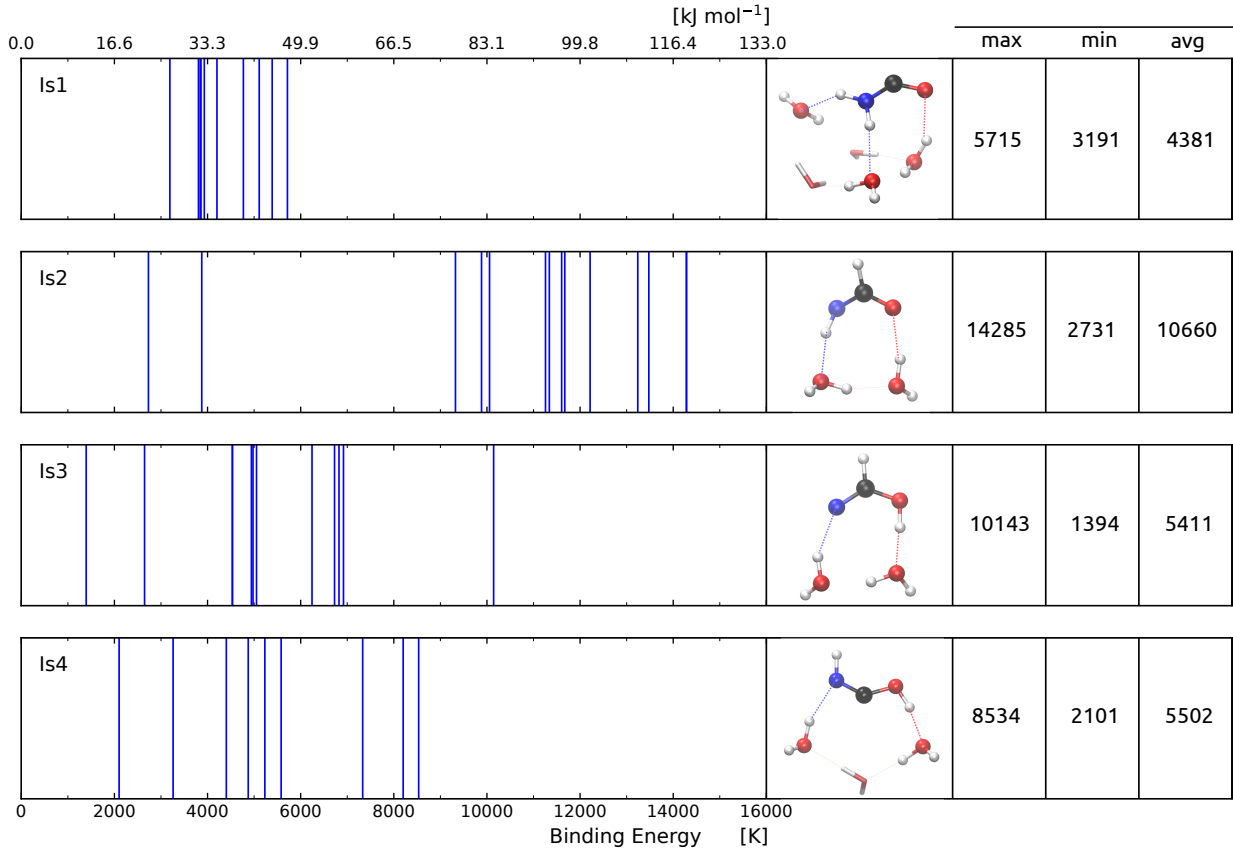


Figure 4: Range of BE calculated in this work for carbamoyl isomers (from top to bottom: Is1–4) adsorbed on a set of small water clusters, $(\text{H}_2\text{O})_{1-5}$. The energy has been computed at ω -PBE-D3BJ/def2-TZVP level of theory, using PWB6K-D3BJ/def2-TZVP geometries. The first column reports the set of BE values obtained for a specific isomer: system optimization and BE calculation are done individually for each binding site, hence the blue lines refer to the BE of a specific Is(1–4)– $(\text{H}_2\text{O})_{1-5}$ structure. The second column reports the structure that provides the highest BE of the set, for all systems. The isomers and the water molecules to whom they are directly interacting with, are represented as balls and sticks, the rest as sticks. The H-bond interactions established by the isomers are highlighted. The remaining columns report the maximum (max), minimum (min) and average (avg) BE values obtained for each set, in K.

In order to estimate the BE of carbamoyl and the other isomers absorbed on ice, we considered a set of minimal water clusters (up to 5 water molecules, $(\text{H}_2\text{O})_{1-5}$). Sampling of the radicals around the clusters, followed by filtering according to geometrical criteria, provided a set of unique binding sites(Is(1–4)– $(\text{H}_2\text{O})_{1-5}$), each of them entailing a specific BE value.

Fig. 4 reports the range of BE calculated for each isomer, along with a image of the structure that provides the highest BE of the set. The largest BEs appear to belong to isomer Is2, with a average BE of around 10600 K. In this isomer there is a possible resonance between the carbonyl and iminic form, in which the unpaired electron is localized on the oxygen. Therefore, the combination of the unpaired electron on the oxygen-end acting as H-bond acceptor and the imine N–H moiety of the molecule acting as H-bond donor, provides strong adsorption of the species on ice. The isomers that present an alcoholic group, Is(3,4), also display similar BEs, centered around 5500 K. Taking into account the structures with the highest BE for these isomers, it can be noticed that the O–H group acts primarily as H-bond donor, while N–H group (in Is4) and the amidic group (in Is3) as H-bond acceptor, meaning that Is(3,4) also present similar adsorption motives. Finally, carbamoyl (Is1) is the radical with the lowest average BE (4381 K). However, analysis of the structures’ geometries revealed that, in the majority of them, the binding does not take place through the C-atom, where the radical is located, which might provide a explanation for the range of lower BE values.

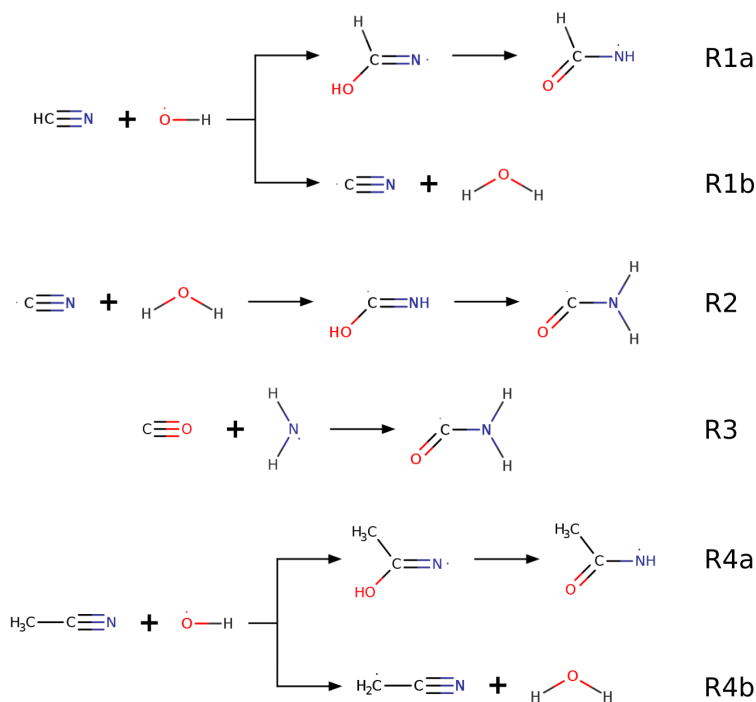
3.3 Formation pathways of carbamoyl isomers

Table 2: Energy barriers (ΔE^\ddagger) and reaction energies (ΔE^o) computed for all of the reactions studied, at BMK-D3BJ/def2-TZVP level of theory, using BHandHLYP-D4/def2-SVP geometries. Values in kJ mol^{-1} .

			Addition		N-H Rotation		Tautomerization		H-Extraction	
			ΔE^\ddagger	ΔE^o						
R1	OH + HCN	Gas-phase	15.6	-130.1	—	—	165.1	8.3	82.7	42.8
		ASW	26.7	-113.8	—	—	68.6	17.3	94.2	3.1
R2	CN + H ₂ O	Gas-phase ^a	172.2	—	130.1	—	190.8	—	—	—
		ASW	70.6	-81.9	38.5	-36.0	6.2	-84.5	—	—
R3	NH ₂ + CO	Gas-phase	10.2	-120.0	—	—	—	—	—	—
		ASW	12.6	-110.8	—	—	—	—	—	—
R4	OH + CH ₃ CN	Gas-phase	19.1	-115.9	—	—	154.6	6.6	32.9	-80.2
		ASW	40.2	-105.1	—	—	59.2	6.9	32.0	-76.9

^a Values from the literature,²⁵ computed at BHYLP/6-311++G(d,p) level of theory and basis.

Scheme 1 shows the reaction pathways studied in this work. Each of them have been simu-



Scheme 1: Reactions pathways studied in this work.

lated using the ASW ice model, while R1, R3 and R4 are studied in gas-phase, as well. For Reactions R1 and R4 we investigated two different outcomes, based on the addition reaction (a) and water elimination (b). Fig. 5 shows the reactive site selected for R(1–4) on ASW. Table 2 reports the energy barriers and reaction energies for all the pathways.

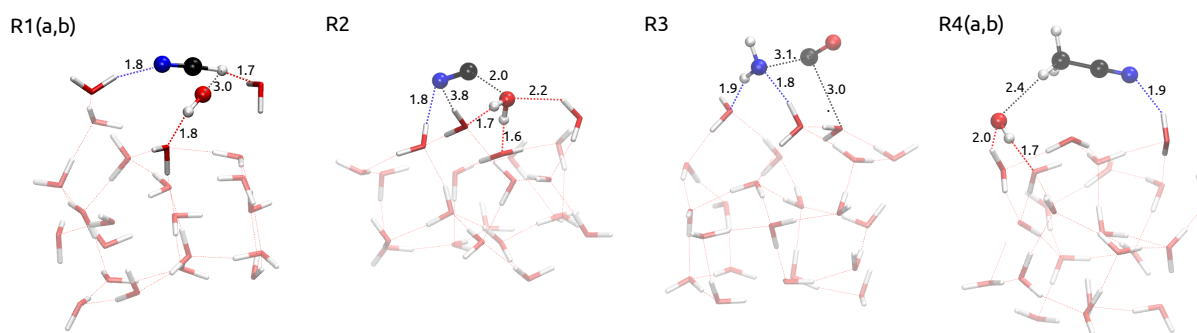


Figure 5: Reactive sites selected for the processes studied in this work. Geometries obtained using BHandHLYP-D4/def2-SVP. The fragments that participate in the reaction are represented as balls and sticks, the rest as sticks. The water molecules that establish H-bond interactions with the reactants are highlighted. Relevant bond distances are reported in Å. The color scheme for the atoms is red for O, black for C, blue for N and white for H.

3.3.1 R1: Gas-phase reaction pathways for OH + HCN

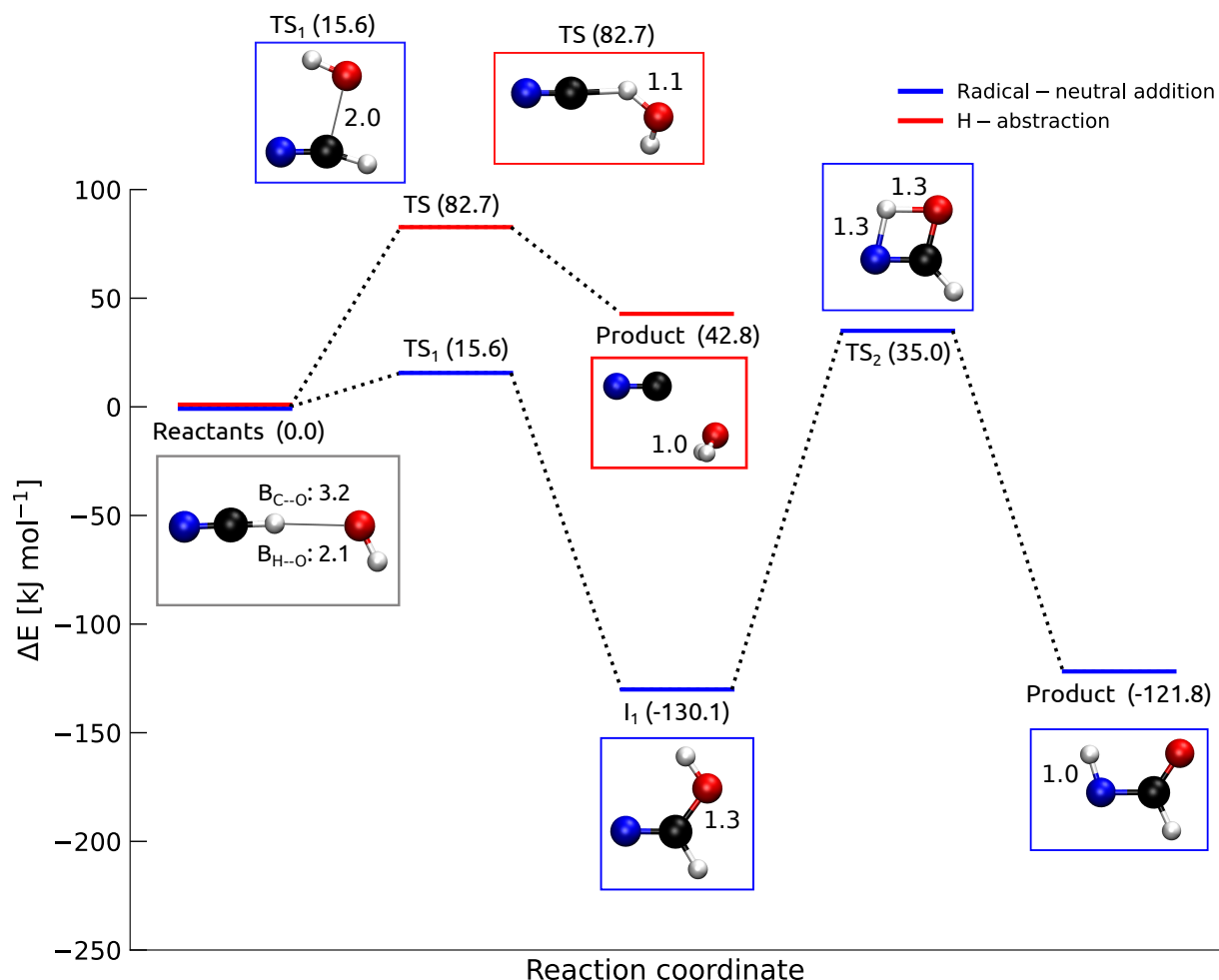


Figure 6: Energy and stationary states for the gas-phase reaction R1: OH + HCN, using BHandHLYP-D4/def2-SVP geometries and BMK-D3BJ/def2-TZVP energies. The process has two possible outcomes: the addition, R1a in blue, and the water elimination, R1b in red. Distances in Å. The color scheme for the atoms is red for O, black for C, blue for N and white for H.

Radical-neutral addition: formation of Is3 and tautomerization from Is3 to Is2: Fig. 6 reports the energy diagram for the reaction. The addition of OH to HCN (Fig. 6, blue pathway) is composed of two steps: the addition step, which entails an energy barrier of 15.6 kJ mol⁻¹ and yields the intermediate imidic radical isomer Is3 (I1, Fig. 6), followed by the tautomerization step (energy barrier of 165.1 kJ mol⁻¹) from isomer Is3 to Is2. It is important to note that for the tautomerization step in the gas-phase, a very strained

configuration is needed for the transition state (TS₂, Fig. 6), resulting in a high TS energy. Furthermore, the intermediate (Is3, methanimidic acid) corresponds to the thermodynamic product, while the amide form the radical (Is2) has slightly higher energy, consistent with the relative energies computed in Sec. 3.1.

H-abstraction: water elimination For the hydrogen abstraction (Fig. 6, red pathway), the reaction presents a significant barrier of 82.7 kJ mol⁻¹, 67.1 kJ mol⁻¹ larger than the barrier of the addition. In light of this result, we conclude that the addition product is the most plausible pathway for this reaction channel in gas-phase.

3.3.2 R1: ASW reaction pathways for OH + HCN

Binding energy distributions and binding modes analysis:

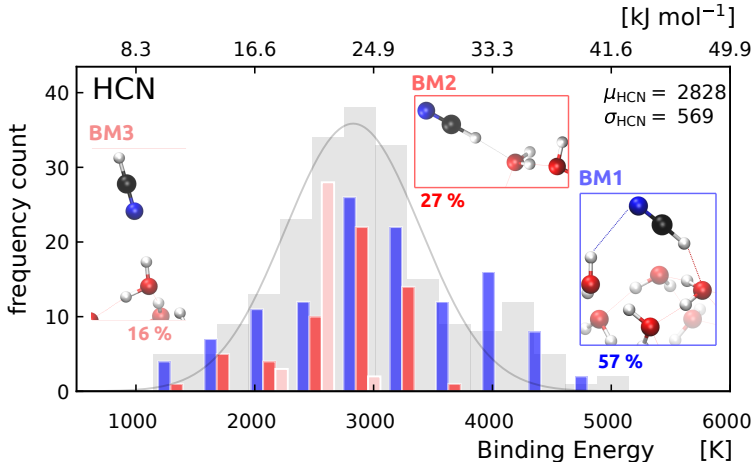


Figure 7: Histogram of the BE distribution of HCN computed on a set-of-clusters model of 22 water molecules, calculated at MPWB1K-D3BJ/def2-TZVP//HF-3c/MINIX level of theory, without including ZPVE correction. BE values are given in K (lower scale) and kJ mol⁻¹ (upper scale). The figure displays a composite plot: the grey histogram refers to the total data, while the structures corresponding to different binding modes (BM1-3) are colored in blue, red and pink. Mean BE (μ) and standard deviations of a Gaussian fit (σ) for the total distribution (grey data) are reported in K. The insets show an example of the different binding modes encountered.

Fig. 7 shows the BE distribution for HCN (upper panel) adsorbed on the set of ASW clusters, in units of Kelvin and kJ mol⁻¹. The distribution contains 212 unique binding sites and

displays a single marked distribution which is slightly asymmetric towards higher energies. The application of a Gaussian fit to the distributions allowed to estimate the mean (μ) and standard deviation (σ). For HCN, μ is 2828 K with σ of 569 K. We have been able to identify three binding modes, based on the analysis of characteristic distances in the adsorption sites. The binding mode that exhibits the highest BE values and also the most common (BM1, 57%, in blue in Fig. 7) is given by the creation of two H-bonds via both the extremities of the molecule. The H-atom act as H-bond donor while the interaction on the side of N-atom is established by one of the surface molecules. The other binding modes present solely one of the H-bond interactions: HCN acting as H-bond donor (BM2, 27%, red) and as H-bond acceptor (BM3, 16%, pink), and show lower BEs, suggesting that both the interactions are paramount to produce strong binding sites. The latter modes consequently display a minor level of insertion into the ice network.

In order for the addition of OH to HCN (R1a) to take place, a C–O bond needs to be established with the central C-atom of HCN, thereby, the backbone of the molecule need to be available for the reaction. Some of BM1 structures, being well inserted in the surface H-bond network, might present steric hindrance, preventing the reaction. On the other hand, in binding sites where the molecules are pointing upward away from the surface (BM2-3), the C-atom is located further away with respect to the surface, making it difficult to reach for a roaming radical. Regarding the H-abstraction from HCN (R1b), apart from BM3 binding sites where the H-extremity is available, the reaction requires the breaking of a H-bond interaction between the molecule and the surface, as well as the breaking of C–H bond, hinting that the process might be favored in sites where the HCN is loosely bound. Such considerations underline the importance of selecting the proper site for the reaction, as the ASW offers a large variety of binding situations, even for a small species like HCN.

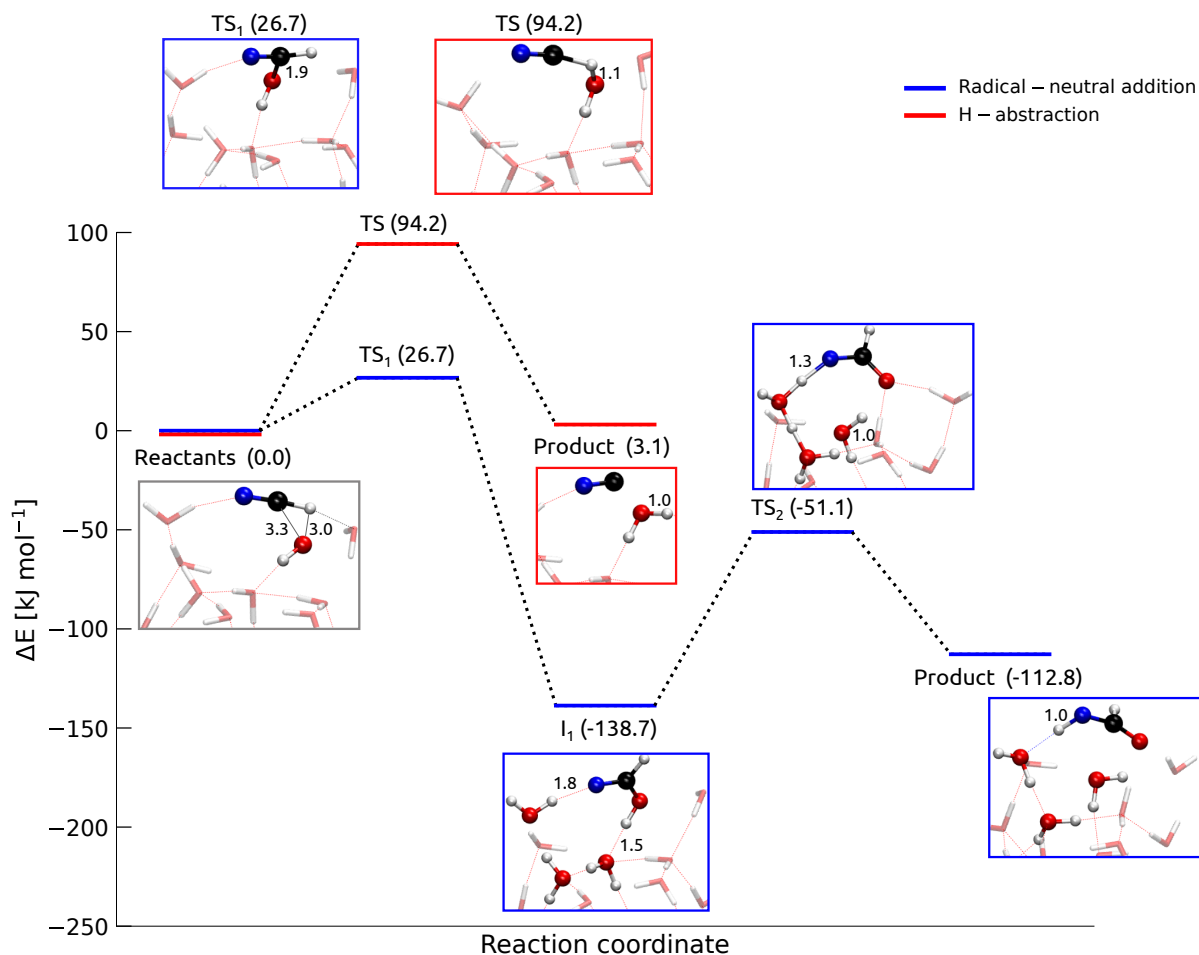


Figure 8: Energy and stationary states for the ASW reaction R1: OH + HCN, using BHandHLYP-D4/def2-SVP geometries and BMK-D3BJ/def2-TZVP energies. The process has two possible outcomes: the addition, R1a in blue, and the water elimination, R1b in red. Distances in Å. The color scheme for the atoms is red for O, black for C, blue for N and white for H.

Radical-neutral addition: formation of Is3 and tautomerization from Is3 to Is2: Fig. 8 shows the energies and stationary states for the OH + HCN for both the addition and hydrogen extraction reactions over the ASW surface. The reactant complex has been obtained following the procedure in Sec. 2.4; as prospective binding site for HCN we selected a high BE structure, belonging to the BM1 binding mode, from the binding mode analysis previously carried out. The reactive site is reported in Fig. 5: the HCN fragment is establishing H-bonds with two surface water molecules, via both its extremities.

For the addition reaction, we also studied the possibility of a tautomerization reaction to transform the imidic-acid tautomer (Is3) to the amide radical (Is2). The OH + HCN addition reaction presents a TS energy of 26.7 kJ mol⁻¹. The resulting imidic-acid intermediate is exothermic with an energy of -138.7 kJ mol⁻¹. The tautomerization reaction from the imidic to the amidic radical (Is3 to Is2) presents a high TS barrier of 68 kJ mol⁻¹. This surface tautomerization reaction involves a proton relay carried out by three surface water molecules, a type of mechanism that has been observed in other isomerization and addition reactions on ASW surface models.^{25,49,50} Furthermore, despite the high barrier, the TS energy remains below that of the OH + HCN reactant complex, indicating that the energy released from the first highly exothermic step could potentially be utilized to overcome this barrier. Finally, it is worth noting that the overall lowest energy state on this PES is the Is3, the imidic-acid radical isomer (Fig. 8, I₁), and the energy difference between the imidic-acid and the amide radical (Is2) is further increased compared to that in the gas-phase.

H-abstraction: The alternative H-abstraction pathway for OH + HCN has a TS barrier of the 94.2 kJ mol⁻¹, which is significantly higher than the addition barrier. On the ASW surface, the products of the H-abstraction reaction are slightly endothermic.

3.3.3 R2: ASW reaction pathway for CN + H₂O

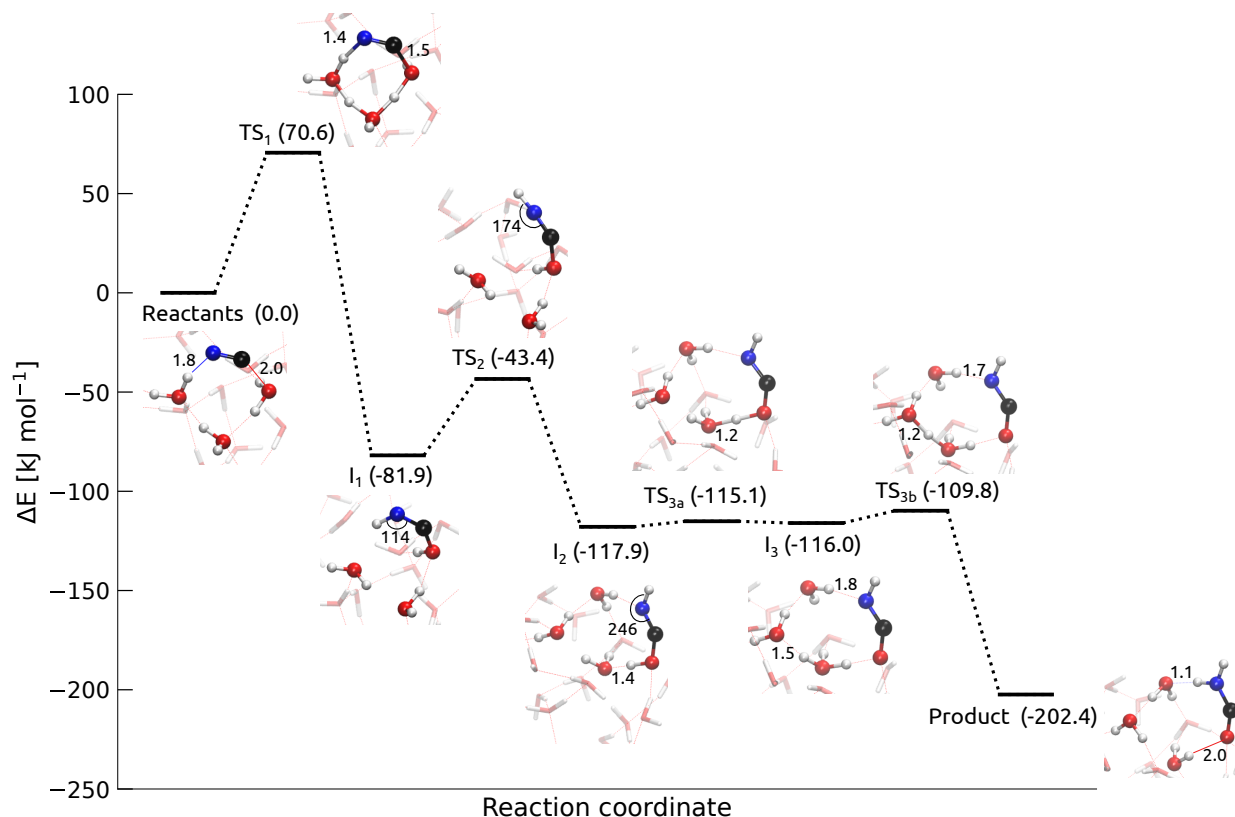


Figure 9: Energy and stationary states for the ASW reaction R2: CN + H₂O, using BHandHLYP-D4/def2-SVP geometries and BMK-D3BJ/def2-TZVP energies. Distances in Å, angles in degree. The color scheme for the atoms is red for O, black for C, blue for N and white for H.

Radical-neutral addition: formation of Is₄ and tautomerization to Is₁: We studied the addition pathway of CN + H₂O. The reactive site structure is reported in Fig. 5, while the PES and the results in terms of stationary point geometries and energies are shown in Fig. 9. The reactive site has been selected according to the binding mode analysis for H₂O molecule carried out in a previous work of our group.³⁶ The binding site of H₂O is of high BE, as the molecule is strongly inserted into the H-bond network of the surface, as it can be noted by the high number of interactions that it is establishing with the neighbouring molecules (highlighted in Fig. 5).

Differently to the reactions of OH with HCN, in this reaction the addition to the surface

water molecule triggers a proton-relay in the first phase of the reaction. This involves a hydrogenation of the N-atom end of the CN radical to yield the isomer Is4 (Fig. 9, I₁) and has therefore a significantly higher reaction barrier than the OH addition to HCN. Furthermore, for the subsequent tautomerization reaction to take place, converting the Is4 isomer to the carbamoyl Is1, a second proton relay is necessary. The conformation of the first intermediate I₁, however, is not oriented properly and in order for the tautomerization to proceed, the N-H group needs to rotate to establish an acceptor H-bond, instead of a donor one. The conformational change (TS₂) presents a barrier of 38.5 kJ mol⁻¹, while the proton relay takes place in two steps (TS_{3a,b}) and displays a very low total barrier of 6.2 kJ mol⁻¹, therefore, the largest barrier in the tautomerization step corresponds to the conformational change in order to achieve the correct arrangement of the reactants.

The differences between our results and the work of Rimola et al.²⁵, presenting a lower net TS barrier of 16.1 kJ mol⁻¹ for the addition and -74.8 kJ mol⁻¹ for the tautomerization, suggest that there might be a significant dependence of the TS energy on the binding site for this reaction. Furthermore, here we presents a different mechanism for the tautomerization, as that part of reaction CN + H₂O is step-wise, while in the work of Rimola et al. it presents a concerted mechanism. Moreover, in said study there was no need for a conformation change, due to the particular choice in the binding site of CN on the ice model. The model used was obtained by fusing two smaller water clusters in order to form a cavity, therefore providing additional H-bond interactions to CN radical. Hence, the peculiar binding of CN within such cavity allowed for two proton-relays to be carried out on the same binding site, since the N-atom was receiving two H-bonds in the reactive site.

3.3.4 R3: ASW reaction pathway for $\text{NH}_2 + \text{CO}$

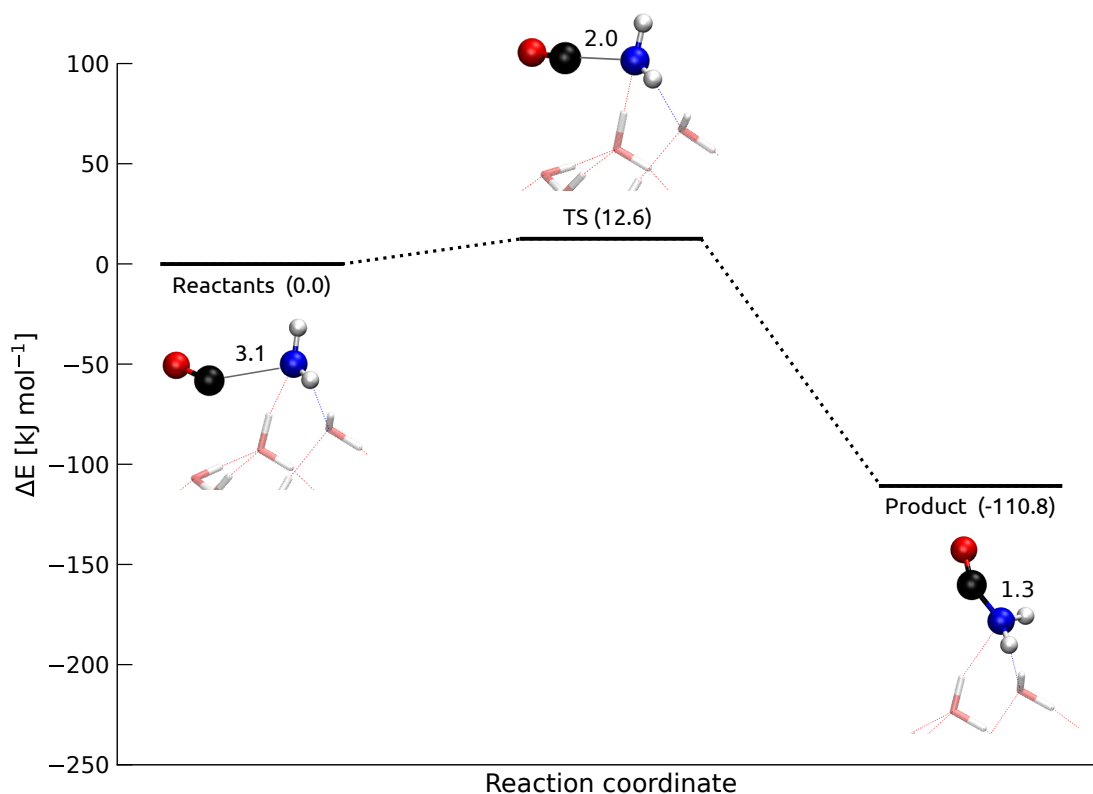


Figure 10: Energy and stationary states for the ASW reaction R3: $\text{NH}_2 + \text{CO}$, using BHandHLYP-D4/def2-SVP geometries and BMK-D3BJ/def2-TZVP energies. Distances in Å. The color scheme for the atoms is red for O, black for C, blue for N and white for H.

We studied the $\text{NH}_2 + \text{CO}$ addition on the ASW model surface, to form the carbamoyl radical (Is1). This reaction is commonly included in astrochemical gas-grain models as a possible surface reaction to the formation of formamide.³³ BE distribution and binding mode analysis for NH_2 have been calculated in a previous work.³⁶ A single binding mode was found, therefore we selected a high-BE site and sampled it with the CO molecule to find a potential reactant complex. Fig. 5 reports the reactive site selected to carry out the reaction on ASW. It can be seen that the NH_2 radical forms two H-bonds with the water surface, one being donated and one received, which determine the strong binding configuration for this species; while CO is not engaging in significant interaction with the surface nor with NH_2 . Figure 10 shows the PES of this reaction. The reaction is concerted and leads to the formation

of carbamoyl Is1. It presents a barrier of 12.6 kJ mol^{-1} (Fig. 10, TS) and a marked exothermic character. This result corresponds to the lowest barrier we encountered in this work for the formation of a carbamoyl isomer on ASW. However, due to the binding mode of the carbamoyl radical product, further tautomerization to the imidic-acid form (Is3) could only be possible after a conformational change that establishes a receiving H-bond to the water surface through the carbonyl end.

3.3.5 R4: Gas-phase reaction pathways for OH + CH₃CN

Finally we probed a reaction pathway for acetamide by assessing the formation of the acetamide N-radical CH₃(C=O)NH precursor.

Radical-neutral addition: formation of the imidic isomer and tautomerization to the amidic form: The gas-phase addition of OH to CH₃CN (Fig.11, blue pathway) follows a similar mechanism to the addition of OH to HCN (R1a, Sec. 3.3.1). The mechanism involved OH addition, giving the imidic radical, CH₃C(OH)N, with a barrier of 19.1 kJ mol^{-1} , followed by the tautomerization to the amidic form: CH₃(C=O)NH, barrier $154.6 \text{ kJ mol}^{-1}$. The barrier for the first step is slightly larger than that of reaction R1a, while the second step presents a smaller barrier by 10.5 kJ mol^{-1} . The latter difference might be attributed the fact that imidic acid intermediate is more constrained than the equivalent state in the HCN + OH reaction pathway, and therefore is closer to TS₂, thus requiring less energy to reach it.

H-abstraction: water elimination The competitive H-abstraction (Fig.11, red pathway) has a barrier of 32.9 kJ mol^{-1} , which is higher than the addition barrier of 19.1 kJ mol^{-1} . Hence, analogously to the OH + HCN case (R1b, Sec. 3.3.1), the addition is the favored outcome for this pathway. However, the reaction barrier is notably smaller (by about 50 kJ mol^{-1}) when compared to R1b. This might be imputed to the fact that the H-atom which is abstracted in R1b belongs to backbone of HCN molecule, while in R4b is part of the methyl group, hence, entailing a different kind of energetic expenditure for the process.

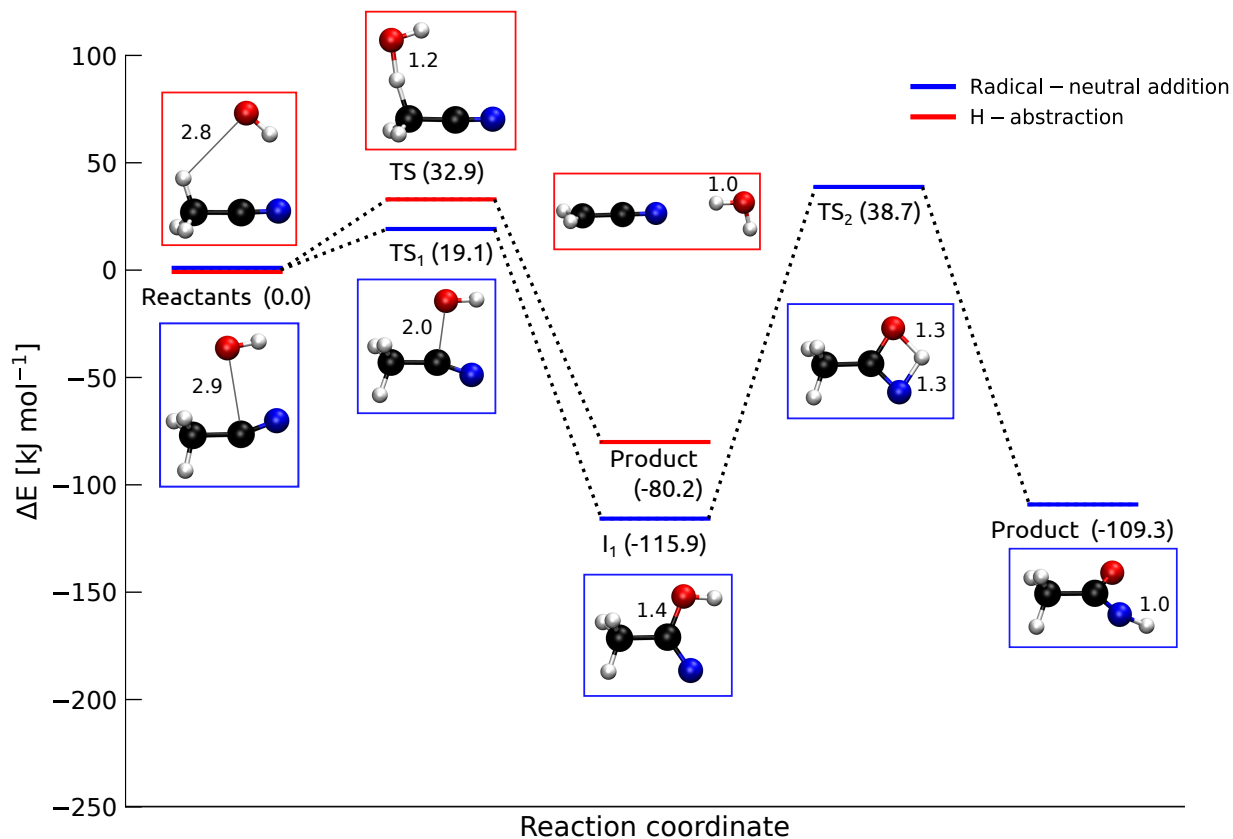


Figure 11: Energy and stationary states for the gas-phase reaction R4: $\text{OH} + \text{CH}_3\text{CN}$, using BHandHLYP-D4/def2-SVP geometries and BMK-D3BJ/def2-TZVP energies. The process has two possible outcomes: the addition, R4a in blue, and the water elimination, R4b in red. Distances in Å. The color scheme for the atoms is red for O, black for C, blue for N and white for H.

3.3.6 R4: ASW reaction pathway for $\text{OH} + \text{CH}_3\text{CN}$

Binding energy distributions and binding modes analysis:

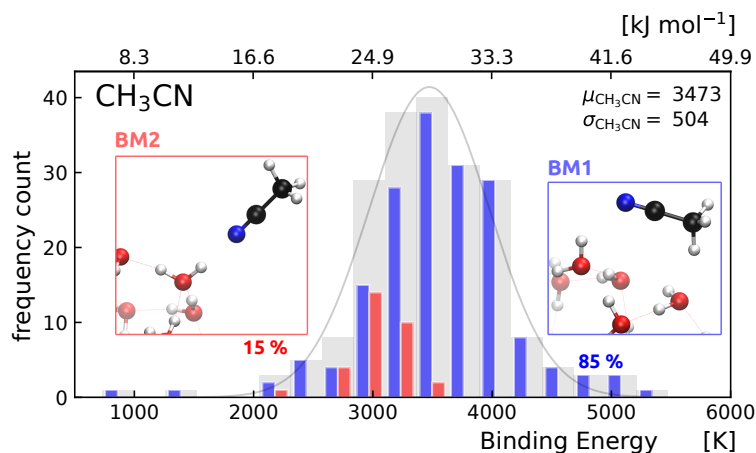


Figure 12: Histogram of the BE distribution of CH_3CN computed on a set-of-clusters model of 22 water molecules, calculated at MPWB1K-D3BJ/def2-TZVP//HF-3c/MINIX level of theory, without including ZPVE correction. BE values are given in K (lower scale) and kJ mol^{-1} (upper scale). The figure displays a composite plot: the grey histogram refers to the total data, while the structures corresponding to different binding modes (BM1-2) are colored in blue and red. Mean BE (μ) and standard deviations of a Gaussian fit (σ) for the total distribution (grey data) are reported in K. The insets show an example of the different binding modes encountered.

Fig. 12 reports the BE distribution of CH_3CN adsorbed on the set of ASW clusters. The distribution contains 204 unique binding sites and its centered around 3473 K, with a standard deviation of 504 K. The μ of the distribution is shifted toward high BE values with respect to HCN by almost 650 K, while the distribution is narrower. Only two binding modes have been identified: one where CH_3CN interacts with the water surface via both sides (BM1, blue, analog to BM1 for HCN), and one where only N=C is accepting a H-bond (BM2, red, analog to BM3 for HCN). We did not detect a third binding mode, where only the methyl group is involved, analog to BM2 for HCN. BM1 structures constitute the vast majority of the binding sites (85%). Furthermore, they represent the middle part and the entire high BE tail of the BE distribution. On the other hand, BM2 structures are mostly located around 3000 K, in correspondence of the analog structures for HCN (BM3 sites), suggesting that, when the methyl is not taking part in the interaction, the two species present a similar adsorption behaviour. Considering the significant difference in the percentage of structures found for the two modes, it is expected for Reaction R4(a,b) to take place in correspondence

of BM1 binding sites.

Radical-neutral addition: formation of the imidic isomer and tautomerization to the amidic form:

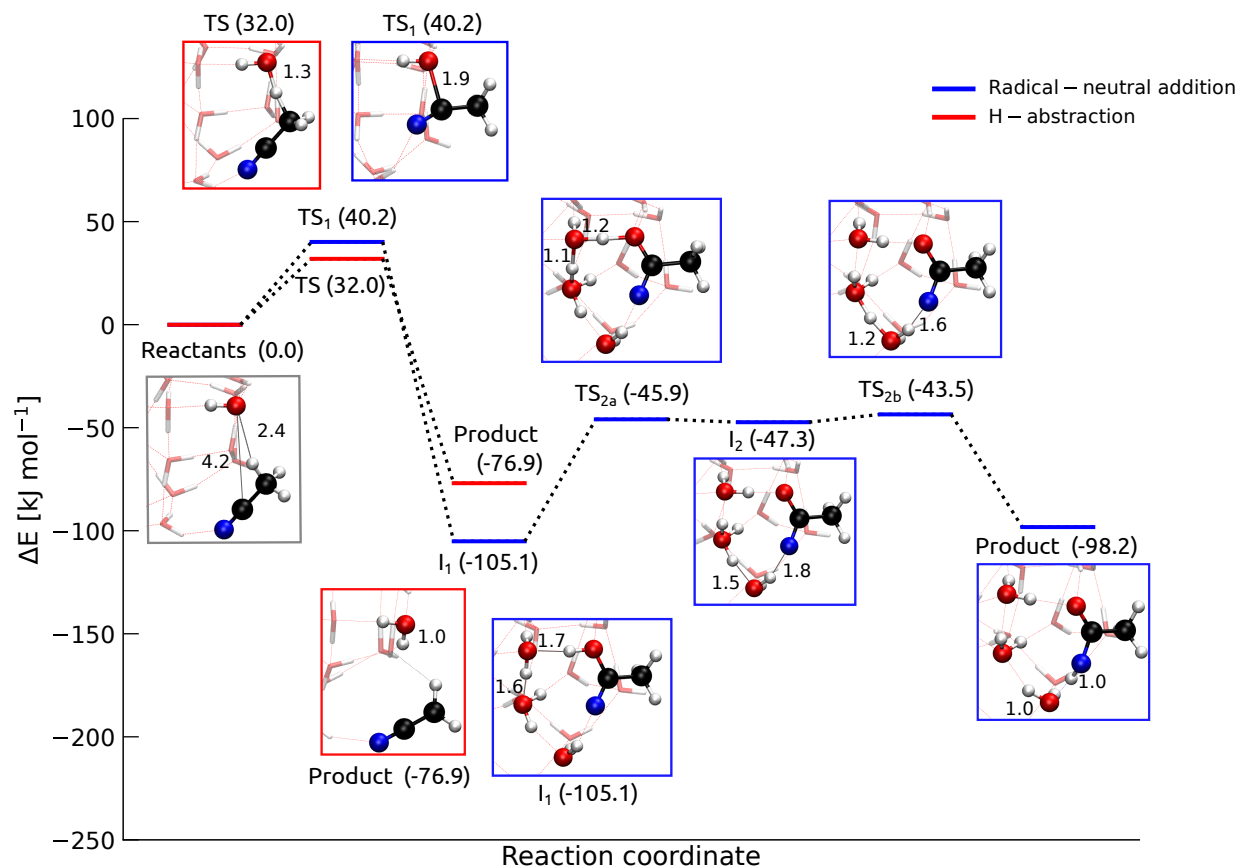


Figure 13: Energy and stationary states for the ASW reaction R4: $\text{OH} + \text{CH}_3\text{CN}$, using BHandHLYP-D4/def2-SVP geometries and BMK-D3BJ/def2-TZVP energies. The process has two possible outcomes: the addition, R4a in blue, and the water elimination, R4b in red. Distances in Å. The color scheme for the atoms is red for O, black for C, blue for N and white for H.

The results for the different reaction channels of the $\text{OH} + \text{CH}_3\text{CN}$ PES are shown in Fig. 13. The reactive site has been obtained by sampling a high-BE structure extracted from CH_3CN distribution. The binding site belongs to BM1 mode, as it can be seen from the H-bond interactions established by both sides of the molecule.

The addition reaction (Fig. 13, blue pathway) presents a TS energy of 40.2 kJ mol^{-1} (Fig. 13, TS₁). The following tautomerization step from the imidic form of the radical (Fig. 13, I₁) to the amidic form (Fig. 13, Product), takes place through a proton-relay involving three water molecules and follows a step-wise mechanism. The additional stationary state that we found with respect to the reaction in gas-phase, corresponds to a dipolar intermediate (Fig. 13, I₂) in which a hydronium ion is created (Fig. 13, TS_{2a}). Subsequently, in the second step of the proton-relay, the hydronium ion transfers the proton (Fig. 13, TS_{2b}), enabling the completion of the tautomerization process. The stage constitute a submerged barrier with a net TS energy of $-45.9 \text{ kJ mol}^{-1}$. Moreover, the step-wise mechanism for the tautomerization results in an lower barrier (59.2 kJ mol^{-1}), compared to the analog stage of R1a (68.6 kJ mol^{-1}). Finally, as it was the case for R1a, the imidic-acid radical isomer (Fig. 13, I₁) is the lowest energy structure on this PES.

H-abstraction: water elimination The energy barrier to the H-abstraction R4b (Fig. 13, red pathway) is 32.0 kJ mol^{-1} . Such value is slightly lower than that of the addition R4a (40.2 kJ mol^{-1}). A possible reason for the lower barrier could be the particularly favorable orientation of the OH radical in the reactant complex on the ASW surface, which facilitates the H-abstraction reaction, since the OH radical is already forming a H-bond to the methyl H-atom. On the other hand, for the addition (R4a) to take place, such H-bond between OH and the methyl group must be broken.

When comparing reaction R4b on ASW to the H-abstraction on ASW in OH + HCN (R1b, Sec. 3.3.2), the H-abstraction emerges as a competitive process, as it displays similar TS energies to the addition reaction R4a, which was not the case for R1b vs R1a. Another difference between R1 and R4 is that R4b is markedly exothermic ($-76.9 \text{ kJ mol}^{-1}$), while R1b was endothermic by 3.1 kJ mol^{-1} .

3.4 Comparison between Gas-phase and ASW reaction pathways

Table 2 reports the energy barriers and reaction energies for the different pathways, carried out in gas-phase and using the ASW surface model.

R1: The addition of OH to HCN (R1a) on ASW sees an increase of the TS energy with respect to the gas-phase of around 10 kJ mol^{-1} (Fig. 8, 6, TS₁). The observed increase appears to stem from the enhanced interaction of the hydroxyl radical with the surface. Such interaction is not present in the gas-phase and must be overcome to facilitate the addition reaction, resulting in a higher TS₁ barrier. On the other hand, the R1a is more exothermic on the ASW surface (-138.7 vs $-130.1 \text{ kJ mol}^{-1}$), indicating that the interaction of Is3 radical with the surface increases the intermediate stability (I₁ in the corresponding figures), with respect to the reactant complex. The tautomerization reaction from the imidic to the amidic radical (Is3 to Is2) on the ASW model presents a significant reduction compared to the gas-phase barrier (TS₂, 68.6 vs $165.1 \text{ kJ mol}^{-1}$, respectively), which is attributed to a change in mechanism, thus submerging the barrier below the reactant energy. Similarly to the addition reaction, carrying out the H-abstraction process (R1b) on ASW requires the breaking of the H-bond established by HCN with the surface, resulting in an increased barrier compared to the gas-phase (94.2 vs 82.7 kJ mol^{-1}). On the ASW surface, the products of R1b are slightly endothermic (3.1 kJ mol^{-1}), albeit much less than in the gas-phase.

R2: In this work, the reaction has been studied solely using the ASW model, therefore, we refer to the literature²⁵ for the energy values calculated in gas-phase. The reaction is the addition of CN to H₂O to form first Is4 radical (TS₁) followed by a conformational change in the isomer configuration (TS₂) allowing for the tautomerization (TS₃) from Is4 to Is1 carbamoyl radical. All the reaction barriers are notably lower on the ASW compared to the gas-phase, by around 100 kJ mol^{-1} for the first two steps, and even more ($184.6 \text{ kJ mol}^{-1}$) for TS₃. The third step is also the one that differs the most in terms of reaction mechanism, as it is concerted in the gas-phase, while it takes place in a step-wise fashion on ASW. The change can be imputed to the fact that in the latter, the tautomerization takes place establishing

a proton-relay that involves three water molecules from the ASW, bridging the proton from one side of the radical to the other. That feature increases the complexity of the process, since the H-bond network of the ice molecules has a important and specific effect of each step of the proton transfer process. Both the reactions in gas-phase and on ASW have a marked exothermic character. In summary, the major difference between R2 carried out in the gas-phase, is constituted by the fact that, on ASW, the barriers for $\text{TS}_{2,3}$ are lowered to such extent that become submerged with respect to the reactant energy, making TS_1 the only barrier to be overcome for the process to take place.

R3: The addition of NH_2 to CO is the process that presents the smallest variations between the gas-phase and the reaction on ASW. In fact, there is no change in the mechanism, and the TS barriers are comparable (12.6 vs 10.2 kJ mol^{-1} for ASW and gas-phase, respectively) as well as the reaction exothermicity (-110.8 vs -120.0 kJ mol^{-1}). This is due to the fact that, in the ASW reactive site, only one of the reactive fragments (NH_2) is interacting with the ice, hence, the TS geometry is mostly unchanged with respect to the gas-phase.

R4: The reaction between OH and CH_3CN presents two possible outcomes. The addition pathway (R4a) on ASW presents a noticeably higher barrier (almost 20 kJ mol^{-1}) than the gas-phase reaction. Such an increase in the TS energy stems from the orientation of the OH radical in the reactive complex, which is aligned towards the methyl group and thus more impeded in forming the C–O bond. Regarding the second step of the reaction (TS_2), the tautomerization of the imidic isomer to the amidic form of the radical, the mechanism changes from concerted in the gas-phase to step-wise on ASW, where the proton transfer takes place via a proton relay involving three water molecules, similarly to what we found for R2. The total barrier for this process (59.2 kJ mol^{-1}) is also much lower than that of the concerted reaction in the gas-phase, by about 100 kJ mol^{-1} . Moreover, we found TS_2 for such pathway to become a submerged barrier, in passing from the gas-phase to ASW, as it was the case for R2. On the other hand, the barrier for the H-abstraction process (R4b), on ASW, is very similar to that in gas-phase (32.0 vs 32.9 kJ mol^{-1}): the aforementioned

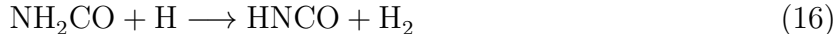
orientation of the OH radical in the reactive complex, which minimizes the distance with the methyl group, results to be particularly favorable for this specific outcome.

4 Astrophysical implications

Based on the results presented in this paper, the addition path OH + HCN to yield the N-radical form of the carbamoyl (Is2), represents an alternative towards amides formation, considering a net reaction barrier of 26.7 kJ/mol (3200 K). Although, the energy barrier makes it unlikely for it to take place in cold dark molecular clouds, the reaction might play a role in later stages of star forming regions. Hence, in the context of this study, a high-BE binding site for HCN makes it more likely to encounter diffusing OH radicals during the warm up phase, before evaporation of the ASW layer.

The selected HCN binding site presented a BE of 4500 K, that is larger than both the OH addition barrier estimated in this work, and the average BE of ASW of 4200 K.⁵¹

Furthermore, we found that the resulting N-radical form of the carbamoyl (Is2), product of OH addition, has an exceptional affinity to the ice surface. Estimation of the BE of such radical on a set of (H₂O)₁₋₅ clusters revealed a average BE of 9931 K, the highest among the carbamoyl isomers considered in this work. Our result suggests that such radical Is2, being more strongly bound to ASW, with respect to carbamoyl (Is1), might survive hydrogenation processes leading to direct generation of formamide (Reaction 1). Such reaction is object of debate,^{16,17} given the competitive channel for the production HNCO:



Moreover, Is2 isomer is linked to another important interstellar amides: radical recombination of Is2 with a CH₃ radical leads to formation of N-methylformamide (Reaction 10).

Taking into account the alternative reactive channel involving H-abstraction from HCN,

leading to water elimination, revealed a considerably higher barrier with respect to OH-addition reaction, by 66.7 kJ/mol. Nevertheless, the reaction might still be viable under interstellar conditions, due to the increase in the reaction rate when considering quantum tunneling effects on the abstracted hydrogen.

The study of the addition of CN radical to a water molecule strongly bound to the ice surface, leading to the formation of H(N=C)OH isomer of carbamoyl (Is4), subsequently converted to Is1, displays a high reaction barrier of 70.6 kJ/mol (8400 K), which makes it overall an unlikely surface route.

Finally the $\text{NH}_2 + \text{CO}$ pathway displays the lowest barrier of all reactions considered in this work for the generation of carbamoyl isomers. The barrier on ASW is 12.6 kJ/mol (1500 K), which is 1000 K lower than the barriers used in astrochemical models that include this reaction.³³ Our result suggests the need to reconsider the treatment of this process in kinetic models, in order to properly account for the surface catalytic effect provided by the ASW ice.

Finally, the analysis of the possible formation pathway for N-radical acetamide precursor ($\text{CH}_3(\text{C}=\text{O})\text{NH}$), via the addition reaction of OH to CH_3CN , resulted to be less viable than the analog reaction between the radical and HCN. The result is imputed to the higher reaction barrier for the process on the ASW surface, due to the influence of H-bond network on OH orientation with respect to CH_3CN molecule, along with the higher affinity of the OH towards the methyl hydrogen of CH_3CN , which favors the H-abstraction competitive outcome. Therefore, the most probable result of the reaction will be the formation of CH_2CN species, rather than the acetamide precursor radical, more so, considering the possibility of tunneling effects. Our results suggest alternative reaction pathways for amides in the interstellar medium. To improve the detection of these amide species with ALMA, it is essential to conduct more detailed studies on their infrared spectrum and millimeter rotational features in the gas phase. Such studies are particularly important in regions where the warmth from newborn stars releases these prebiotic precursors into the gas phase. Moreover, the high

average binding energies of the resulting amide radicals and the absence of amide observations in cold prestellar cores, suggest that the amides and its precursors would remain frozen out onto the grain surface until the warming up phase of the protostellar core, where they have been detected. Future surveys utilizing the James Webb Space Telescope (JWST), with its exceptional resolution, could facilitate the integration of experimental data with observational findings.

5 Conclusions

In this work, we explored different radical-neutral formation pathways towards simple interstellar amides, on a model ASW surface, through the formation of carbamoyl NH_2CO radical isomers. We computed the relative energy of four carbamoyl isomers in the gas-phase and obtained a range of binding energies for the isomers adsorbed on small water clusters $(\text{H}_2\text{O})_{(1-5)}$. We evaluated, by means of DFT, the binding energy distribution of the reactant molecules HCN and CH_3CN on a ASW set-of-cluster model consisting of 22-water molecules each, and analyzed the different binding modes to select a high binding energy binding mode to study the OH addition reactions. The main conclusions that can be drawn from this study are the following:

1. In the gas-phase, the lowest energy isomer of the NH_2CO radical family is the C-radical carbamoyl (isomer Is1, Fig.1), at the UCCSD(T)-F12/cc-PVDZ-F12 level of theory
2. The isomer with the highest average BE is the N-radical form $(\text{NH}(\text{C}=\text{O})\text{H})$, isomer Is2, Fig.1). Surprisingly, carbamoyl (NH_2CO , Is1), displays the lowest binding energy. This suggests a markedly different stability profile for both radicals on an ice surface, when compared to the gas-phase. More detailed analysis of the adsorption motives of such species on the ASW surface is the object of a forthcoming study.
3. The OH + HCN addition pathway, resulting in the imidic form of the carbamoyl radical, followed by the tautomerization to the N-radical form (Is3 to Is2), appears

to be a feasible formation pathway for formamide and N-methylformamide. In fact, the barrier for OH addition is lower than the binding energy of HCN in the reactive site, such that reactive encounters with diffusing OH radicals might take place under interstellar condition akin to those of star-forming regions.

4. The reaction of CN radical with a water molecule belonging to the ASW surface, displays a high reaction barrier, making this pathway unlikely to take place even in warmer star-forming region.
5. The addition reaction of NH_2 to CO is the energetically most favorable formation route for the generation of carbamoyl NH_2CO , with a modest activation barrier of 12.6 kJ mol^{-1} (1500 K). This barrier is 1000 K lower than the barrier currently used in astrochemical models, suggesting the need to update this value in future models.
6. The formation of acetamide precursor through the addition reaction of OH-radicals to CH_3CN , seems unlikely to take place on ASW surface. We found the barrier to the formation of the imidic radical intermediate ($\text{CH}_3\text{C}(\text{OH})\text{N}$) to be significantly higher than the corresponding gas-phase barrier, resulting in a anti-catalytic behaviour of the ASW surface. Moreover, the lower TS energy displayed by the competitive H-abstraction reaction channel, makes the formation of the radical species (CH_2CN) the most plausible outcome.

These findings suggest potential alternative pathways for the formation of amides through the generation of various isomers of carbamoyl (NH_2CO) radical. However, examining the stability of the different isomers with respect to hydrogenation and methylation on ASW will be pivotal to shed light on the role of such radical precursors in the chemistry of interstellar amides.

Acknowledgement

SVG thanks VRID research grant 2022000507INV for financing this project. GMB gratefully acknowledges support from ANID Beca de Doctorado Nacional 21200180. GSV thanks the Universidad de Concepcin for the Beca de Excelencia Acadmica scholarship. NR thanks FONDECYT POSTDOCTORADO grant 3230221 for financial support.

Supporting Information Available

Supporting Information: XYZ coordinates of all the stationary points reported in this work.

References

- (1) McClure, M. K. et al. An Ice Age JWST inventory of dense molecular cloud ices. *Nature Astronomy* **2023**, *7*, 431–443, Number: 4 Publisher: Nature Publishing Group.
- (2) Portugal, W.; Pilling, S.; Boduch, P.; Rothard, H.; Andrade, D. P. P. Radiolysis of amino acids by heavy and energetic cosmic ray analogues in simulated space environments: -glycine zwitterion form. *Monthly Notices of the Royal Astronomical Society* **2014**, *441*, 3209–3225.
- (3) Lpez-Sepulcre, A.; Balucani, N.; Ceccarelli, C.; Codella, C.; Dulieu, F.; Theul, P. Interstellar Formamide (NH₂CHO), a Key Prebiotic Precursor. *ACS Earth and Space Chemistry* **2019**, *3*, 2122–2137, Publisher: American Chemical Society.
- (4) Colzi, L.; Rivilla, V. M.; Beltrn, M. T.; Jimnez-Serra, I.; Mininni, C.; Melosso, M.; Cesaroni, R.; Fontani, F.; Lorenzani, A.; Snchez-Monge, A.; Viti, S.; Schilke, P.; Testi, L.; Alonso, E. R.; Kolesnikov, L. The GUAPOS project - II. A comprehensive study of peptide-like bond molecules. *Astronomy & Astrophysics* **2021**, *653*, A129, Publisher: EDP Sciences.

- (5) Ligterink, N. F. W.; El-Abd, S. J.; Brogan, C. L.; Hunter, T. R.; Remijan, A. J.; Garrod, R. T.; McGuire, B. M. The Family of Amide Molecules toward NGC 6334I. *The Astrophysical Journal* **2020**, *901*, 37, Publisher: American Astronomical Society.
- (6) Ligterink, N. F. W.; Ahmadi, A.; Luitel, B.; Coutens, A.; Calcutt, H.; Tychoniec, .; Linnartz, H.; Jrgensen, J. K.; Garrod, R. T.; Bouwman, J. The prebiotic molecular inventory of Serpens SMM1: II. The building blocks of peptide chains. 2022; <http://arxiv.org/abs/2202.09640>, arXiv:2202.09640 [astro-ph].
- (7) Zeng, S.; Rivilla, V. M.; Jimnez-Serra, I.; Colzi, L.; Martn-Pintado, J.; Tercero, B.; deVicente, P.; Martn, S.; Requena-Torres, M. A. Amides inventory towards the G+0.6930.027 molecular cloud. *Monthly Notices of the Royal Astronomical Society* **2023**, *523*, 1448–1463.
- (8) Ligterink, N. F. W.; Ahmadi, A.; Luitel, B.; Coutens, A.; Calcutt, H.; Tychoniec, .; Linnartz, H.; Jrgensen, J. K.; Garrod, R. T.; Bouwman, J. The Prebiotic Molecular Inventory of Serpens SMM1: II. The Building Blocks of Peptide Chains. *ACS Earth and Space Chemistry* **2022**, *6*, 455–467, Publisher: American Chemical Society.
- (9) Sanz-Novo, M.; Belloche, A.; Rivilla, V. M.; Garrod, R. T.; Alonso, J. L.; Redondo, P.; Barrientos, C.; Kolesnikov, L.; Valle, J. C.; Rodrguez-Almeida, L.; Jimenez-Serra, I.; Martn-Pintado, J.; Mller, H. S. P.; Menten, K. M. Toward the limits of complexity of interstellar chemistry: Rotational spectroscopy and astronomical search for n- and i-butanal. *Astronomy & Astrophysics* **2022**, *666*, A114, Publisher: EDP Sciences.
- (10) Bisschop, S. E.; Jrgensen, J. K.; van Dishoeck, E. F.; de Wachter, E. B. M. Testing grain-surface chemistry in massive hot-core regions. *Astronomy & Astrophysics* **2007**, *465*, 913–929.
- (11) Lpez-Sepulcre, A.; Jaber, A. A.; Mendoza, E.; Lefloch, B.; Ceccarelli, C.; Vastel, C.; Bachiller, R.; Cernicharo, J.; Codella, C.; Kahane, C.; Kama, M.; Tafalla, M. Shedding

- light on the formation of the pre-biotic molecule formamide with ASAI. *Monthly Notices of the Royal Astronomical Society* **2015**, *449*, 2438–2458, arXiv:1502.05762 [astro-ph].
- (12) Hubbard, J. S.; Voecks, G. E.; Hobby, G. L.; Ferris, J. P.; Williams, E. A.; Nico- dem, D. E. Ultraviolet-gas phase and -photocatalytic synthesis from CO and NH₃. *Journal of Molecular Evolution* **1975**, *5*, 223–241.
- (13) Agarwal, V. K.; Schutte, W.; Greenberg, J. M.; Ferris, J. P.; Briggs, R.; Connor, S.; Van de Bult, C. P. E. M.; Baas, F. Photochemical reactions in interstellar grains photo- lysis of co, NH₃, and H₂O. *Origins of life and evolution of the biosphere* **1985**, *16*, 21–40.
- (14) Ligterink, N. F. W.; TerwisschavanScheltinga, J.; Taquet, V.; Jrgensen, J. K.; Cazaux, S.; vanDishoeck, E. F.; Linnartz, H. The formation of peptide-like molecules on interstellar dust grains. *Monthly Notices of the Royal Astronomical Society* **2018**, *480*, 3628–3643.
- (15) Chuang, K.-J.; Jger, C.; Krasnokutski, S. A.; Fulvio, D.; Henning, T. Formation of the Simplest Amide in Molecular Clouds: Formamide (NH₂CHO) and Its Derivatives in H₂ O-rich and CO-rich Interstellar Ice Analogs upon VUV Irradiation. *The Astrophysical Journal* **2022**, *933*, 107.
- (16) Noble, J. A.; Theule, P.; Congiu, E.; Dulieu, F.; Bonnin, M.; Bassas, A.; Duvernay, F.; Danger, G.; Chiavassa, T. Hydrogenation at low temperatures does not always lead to saturation: the case of HNCO. *Astronomy & Astrophysics* **2015**, *576*, A91.
- (17) Haupa, K. A.; Tarczay, G.; Lee, Y.-P. Hydrogen Abstraction/Addition Tunneling Re- actions Elucidate the Interstellar H₂ NCHO/HNCO Ratio and H₂ Formation. *Journal of the American Chemical Society* **2019**, *141*, 11614–11620.
- (18) Slate, E. C. S.; Barker, R.; Euesden, R. T.; Revels, M. R.; Meijer, A. J. H. M. Compu-

- tational studies into urea formation in the interstellar medium. *Monthly Notices of the Royal Astronomical Society* **2020**, *497*, 5413–5420.
- (19) Belloche, A.; Meshcheryakov, A. A.; Garrod, R. T.; Ilyushin, V. V.; Alekseev, E. A.; Motiyenko, R. A.; Marguls, L.; Mller, H. S. P.; Menten, K. M. Rotational spectroscopy, tentative interstellar detection, and chemical modeling of N-methylformamide. *Astronomy & Astrophysics* **2017**, *601*, A49, Publisher: EDP Sciences.
- (20) Belloche, A.; Garrod, R. T.; Mller, H. S. P.; Menten, K. M.; Medvedev, I.; Thomas, J.; Kisiel, Z. Re-exploring Molecular Complexity with ALMA (ReMoCA): interstellar detection of urea. *Astronomy & Astrophysics* **2019**, *628*, A10, Publisher: EDP Sciences.
- (21) Garrod, R. T.; Jin, M.; Matis, K. A.; Jones, D.; Willis, E. R.; Herbst, E. Formation of Complex Organic Molecules in Hot Molecular Cores through Nondiffusive Grain-surface and Ice-mantle Chemistry. *The Astrophysical Journal Supplement Series* **2022**, *259*, 1, Publisher: The American Astronomical Society.
- (22) Hudson, R. L.; Moore, M. H. New experiments and interpretations concerning the “XCN” band in interstellar ice analogues. *Astronomy and Astrophysics* **2000**, *357*, 787–792, ADS Bibcode: 2000A&A...357..787H.
- (23) Bredehft, J. H.; Bhler, E.; Schmidt, F.; Borrmann, T.; Swiderek, P. Electron-Induced Synthesis of Formamide in Condensed Mixtures of Carbon Monoxide and Ammonia. *ACS Earth and Space Chemistry* **2017**, *1*, 50–59.
- (24) Gerakines, P.; Moore, M.; Hudson, R. Ultraviolet photolysis and proton irradiation of astrophysical ice analogs containing hydrogen cyanide. *Icarus* **2004**, *170*, 202–213.
- (25) Rimola, A.; Skouteris, D.; Balucani, N.; Ceccarelli, C.; Enrique-Romero, J.; Taquet, V.; Ugliengo, P. Can Formamide Be Formed on Interstellar Ice? An Atomistic Perspective. *ACS Earth and Space Chemistry* **2018**, *2*, 720–734, Publisher: American Chemical Society.

- (26) Hama, T.; Watanabe, N. Surface Processes on Interstellar Amorphous Solid Water: Adsorption, Diffusion, Tunneling Reactions, and Nuclear-Spin Conversion. *Chemical Reviews* **2013**, *113*, 8783–8839, Publisher: American Chemical Society.
- (27) He, J.; Frank, P.; Vidali, G. Interaction of hydrogen with surfaces of silicates: single crystal vs. amorphous. *Physical Chemistry Chemical Physics* **2011**, *13*, 15803–15809, Publisher: The Royal Society of Chemistry.
- (28) Noble, J. A.; Congiu, E.; Dulieu, F.; Fraser, H. J. Thermal desorption characteristics of CO, O₂ and CO₂ on non-porous water, crystalline water and silicate surfaces at submonolayer and multilayer coverages. *Monthly Notices of the Royal Astronomical Society* **2012**, *421*, 768–779, Publisher: Oxford Academic.
- (29) Grassi, T.; Bovino, S.; Caselli, P.; Bovolenta, G.; Vogt-Geisse, S.; Ercolano, B. A novel framework for studying the impact of binding energy distributions on the chemistry of dust grains. *Astronomy & Astrophysics* **2020**, *643*, A155, Publisher: EDP Sciences.
- (30) Bovolenta, G.; Bovino, S.; Vhringer-Martinez, E.; Saez, D. A.; Grassi, T.; Vogt-Geisse, S. High level ab initio binding energy distribution of molecules on interstellar ices: Hydrogen fluoride. *Molecular Astrophysics* **2020**, 100095.
- (31) Galano, A. Mechanism of OH Radical Reactions with HCN and CH₃CN: OH Regeneration in the Presence of O₂. *The Journal of Physical Chemistry A* **2007**, *111*, 5086–5091, Publisher: American Chemical Society.
- (32) Bunkan, A. J. C.; Liang, C.-H.; Pilling, M. J.; Nielsen, C. J. Theoretical and experimental study of the OH radical reaction with HCN. *Molecular Physics* **2013**, *111*, 1589–1598, Publisher: Taylor & Francis eprint: <https://doi.org/10.1080/00268976.2013.802036>.
- (33) Garrod, R. T. A THREE-PHASE CHEMICAL MODEL OF HOT CORES: THE FOR-

- MATION OF GLYCINE. *The Astrophysical Journal* **2013**, *765*, 60, Publisher: IOP Publishing.
- (34) Tsuge, M.; Watanabe, N. Behavior of Hydroxyl Radicals on Water Ice at Low Temperatures. *Accounts of Chemical Research* **2021**, *54*, 471–480, Publisher: American Chemical Society.
- (35) Miyazaki, A.; Tsuge, M.; Hidaka, H.; Nakai, Y.; Watanabe, N. Direct Determination of the Activation Energy for Diffusion of OH Radicals on Water Ice. *The Astrophysical Journal Letters* **2022**, *940*, L2.
- (36) Bovolenta, G. M.; Vogt-Geisse, S.; Bovino, S.; Grassi, T. Binding Energy Evaluation Platform: A Database of Quantum Chemical Binding Energy Distributions for the Astrochemical Community. *The Astrophysical Journal Supplement Series* **2022**, *262*, 17, Publisher: The American Astronomical Society.
- (37) Shingledecker, C. N.; Vogt-Geisse, S.; Mifsud, D. V.; Ioppolo, S. In *Astrochemical Modeling*; Bovino, S., Grassi, T., Eds.; Elsevier, 2024; pp 71–115.
- (38) Sure, R.; Grimme, S. Corrected small basis set Hartree-Fock method for large systems. *Journal of Computational Chemistry* **2013**, *34*, 1672–1685, reprint: <https://onlinelibrary.wiley.com/doi/pdf/10.1002/jcc.23317>.
- (39) Zhao, Y.; Truhlar, D. G. Hybrid Meta Density Functional Theory Methods for Thermochemistry, Thermochemical Kinetics, and Noncovalent Interactions: The MPW1B95 and MPWB1K Models and Comparative Assessments for Hydrogen Bonding and van der Waals Interactions. *The Journal of Physical Chemistry A* **2004**, *108*, 6908–6918.
- (40) Weigend, F.; Ahlrichs, R. Balanced basis sets of split valence, triple zeta valence and quadruple zeta valence quality for H to Rn: Design and assessment of accuracy. *Physical Chemistry Chemical Physics* **2005**, *7*, 3297.

- (41) Grimme, S.; Ehrlich, S.; Goerigk, L. Effect of the damping function in dispersion corrected density functional theory. *Journal of Computational Chemistry* **2011**, *32*, 1456–1465.
- (42) Seritan, S.; Bannwarth, C.; Fales, B. S.; Hohenstein, E. G.; Isborn, C. M.; Kokkila-Schumacher, S. I. L.; Li, X.; Liu, F.; Luehr, N.; Snyder Jr., J. W.; Song, C.; Titov, A. V.; Ufimtsev, I. S.; Wang, L.-P.; Martinez, T. J. TeraChem: A graphical processing unit-accelerated electronic structure package for large-scale ab initio molecular dynamics. *WIREs Computational Molecular Science* **2021**, *11*, e1494, _eprint: <https://onlinelibrary.wiley.com/doi/pdf/10.1002/wcms.1494>.
- (43) Turney, J. M. et al. Psi4: an open-source ab initio electronic structure program. *WIREs Computational Molecular Science* **2012**, *2*, 556–565, _eprint: <https://onlinelibrary.wiley.com/doi/pdf/10.1002/wcms.93>.
- (44) Smith, D. G. A.; Altarawy, D.; Burns, L. A.; Welborn, M.; Naden, L. N.; Ward, L.; Ellis, S.; Pritchard, B. P.; Crawford, T. D. The MolSSI QCArchive project: An open-source platform to compute, organize, and share quantum chemistry data. *WIREs Computational Molecular Science* **2021**, *11*, e1491, _eprint: <https://onlinelibrary.wiley.com/doi/pdf/10.1002/wcms.1491>.
- (45) Wang, L.-P.; Song, C. Geometry optimization made simple with translation and rotation coordinates. *The Journal of Chemical Physics* **2016**, *144*, 214108.
- (46) Becke, A. D. A new mixing of HartreeFock and local density-functional theories. *The Journal of Chemical Physics* **1993**, *98*, 1372–1377.
- (47) Boese, A. D.; Martin, J. M. L. Development of density functionals for thermochemical kinetics. *The Journal of Chemical Physics* **2004**, *121*, 3405–3416.
- (48) Warden, C. E.; Smith, D. G. A.; Burns, L. A.; Bozkaya, U.; Sherrill, C. D. Efficient and automated computation of accurate molecular geometries using focal-point approxima-

- tions to large-basis coupled-cluster theory. *The Journal of Chemical Physics* **2020**, *152*, 124109, Publisher: American Institute of Physics.
- (49) Woon, D. E. Ab initio quantum chemical studies of reactions in astrophysical ices. 4. Reactions in ices involving HCOOH, CH₂NH, HCN, HNC, NH₃, and H₂O. *International Journal of Quantum Chemistry* **2002**, *88*, 226–235.
- (50) Baiano, C.; Lupi, J.; Barone, V.; Tasinato, N. Gliding on Ice in Search of Accurate and Cost-Effective Computational Methods for Astrochemistry on Grains: The Puzzling Case of the HCN Isomerization. *Journal of Chemical Theory and Computation* **2022**, *18*, 3111–3121, Publisher: American Chemical Society.
- (51) Tinacci, L.; Germain, A.; Pantaleone, S.; Ceccarelli, C.; Balucani, N.; Ugliengo, P. Theoretical Water Binding Energy Distribution and Snowline in Protoplanetary Disks. *The Astrophysical Journal* **2023**, *951*, 32.

TOC Graphic

